Spatially representative velocity measurement over water-worked gravel beds

James R. Cooper[1] and Simon J. Tait[1]

Received 31 July 2009; revised 29 June 2010; accepted 17 August 2010; published 25 November 2010.

[1] Recent studies have examined the spatial heterogeneity of velocity fields over natural river boundaries. A key challenge is understanding how many velocity measurements are required to provide spatially representative estimates of the flow. This paper describes a series of laboratory experiments in which flow velocities have been measured in a detailed spatial pattern over two water-worked gravel beds. These data have been utilized to deduce the minimum density of measurements required to provide representative estimates of several spatially averaged flow parameters. This was coupled with an investigation into the influence of measurement density on the level of error in the estimation of these parameters. Empirical relationships are developed that can be used to estimate, a priori, the required minimum measurement density for a known precision and accuracy over macroscopically flat, water-worked gravel beds within a range of submergences. These estimates can be based on measurements of the bed roughness length scale, bed shear velocity, and flow depth alone. For all of the flow parameters, the level of error in adopting a lower measurement density than the required minimum, and its change with measurement density, was especially large at the lower densities. Given this dependence on measurement density, caution should be taken when comparing flow estimates from studies that have used similar flow and bed conditions but different measurement densities.

Citation: Cooper, J. R., and S. J. Tait (2010), Spatially representative velocity measurement over water-worked gravel beds, *Water Resour. Res.*, *46*, W11559, doi:10.1029/2009WR008465.

1. Introduction

[2] A number of studies have shown that turbulent flows over water-worked gravel beds are spatially heterogeneous and display evidence of three-dimensionality [e.g., *Lamarre and Roy*, 2005; *Buffin-Bélanger et al.*, 2006; *Legleiter et al.*, 2007; *Cooper and Tait*, 2008; *Hardy et al.*, 2009]. For example, several studies have reported the existence of vortically based, depth-scale flow structures over water-worked gravel surfaces [e.g., *Buffin-Bélanger et al.*, 2000; *Shvidchenko and Pender*, 2001; *Roy et al.*, 2004]. A key challenge is being able to sample adequately this spatial variability. For example, the development of photogrammetric and laser scanning methods for obtaining detailed bed elevation data [e.g., *Butler et al.*, 2002; *Marion et al.*, 2003; *Hodge et al.*, 2009] has led to attempts to produce a spatially integrated roughness coefficient for gravel-bed rivers [e.g., *Furbish*, 1987; *Robert*, 1988, 1990, 1991; *Clifford et al.*, 1992; *Nikora et al.*, 1998; *Butler et al.*, 2001; *Aberle and Smart*, 2003; *Aberle and Nikora*, 2006]. However, it is only possible to exploit these new roughness characterization techniques into flow resistance models if these coefficients can be linked to flow parameters which describe statistically the spatial heterogeneity in the flow.

[3] There is an increasing interest in understanding how flow spatial variability can influence other physical processes occurring within gravel-bed rivers. For example, studies have observed spatial variability in bedload transport [e.g., *Bridge and Jarvis*, 1982; *Ashworth and Ferguson*, 1986; *Radice et al.*, 2009], suspended sediment transport and solute transport [e.g. *Packman et al.*, 2004; *Boxall and Guymer*, 2007; *Tonina and Buffington*, 2007], and ecological structure [e.g., *Bouckaert and Davis*, 1998; *Matthaei and Huber*, 2002; *Lancaster et al.*, 2006]. It has therefore become important to gather spatial information on the flows over water-worked gravel beds.

[4] Single-point velocity measurements describe flow quantities at one location. Thus, it is not possible to link explicitly spatially averaged parameters, whether of the fluid, the boundary, or sediment/solute flux, to these flow properties derived from single-point measurements. This requirement has led researchers to consider how many "single point" velocity measurements are required to provide statistically representative estimates of the spatial properties of a turbulent flow.

[5] *Nikora et al.* [2001] proposed a theoretical framework which could be used to account explicitly for flow spatial variability and to derive spatially averaged flow parameters. This was based on the concept of spatial averaging, which originally had its roots in multiphase and porous media hydrodynamics. It was introduced for studying atmospheric flows by *Wilson and Shaw* [1977], in hydraulics by *Smith and McLean* [1977], and by *Giménez-Curto and Corniero* [1996] for oscillating flow. The framework stated that the time-averaging of the Navier-Stokes equation should be supple-

[1]School of Engineering, Design and Technology, University of Bradford, Bradford, United Kingdom.

0043-1397/10/2009WR008465

Table 1. A Summary of the Experimental Conditions, Where U Denotes the Unimodal Bed, B Denotes the Bimodal Bed, S is the Bed Slope, Q is the Flow Discharge, h is the Flow Depth, k is the Geometric Roughness Height and $\overline{U}$ is the Average Flow Velocity

Run	S	Q(m^3/s)	h(m)	h/k	$\overline{U}$(m/s)
1U	0.00285	0.00159	0.0181	1.2	0.18
2U	0.00285	0.00389	0.0286	1.9	0.27
3U	0.00285	0.00635	0.0395	2.6	0.32
4U	0.00285	0.00869	0.0484	3.2	0.36
5U	0.00285	0.0140	0.0628	4.1	0.45
6U	0.00285	0.0280	0.0900	5.9	0.62
7U	0.00375	0.0162	0.0635	4.2	0.51
8U	0.00375	0.0114	0.0482	3.2	0.47
9U	0.00465	0.0123	0.0492	3.2	0.50
10U	0.00555	0.00978	0.0399	2.6	0.49
11U	0.00645	0.00692	0.0335	2.2	0.41
12U	0.00735	0.00655	0.0295	1.9	0.44
1B	0.00284	0.00143	0.0173	1.3	0.16
2B	0.00284	0.00276	0.0272	2.0	0.20
3B	0.00284	0.00527	0.0373	2.7	0.28
4B	0.00284	0.00809	0.0455	3.3	0.36
5B	0.00284	0.0127	0.0595	4.3	0.43
6B	0.00284	0.0245	0.0845	6.2	0.58
7B	0.00374	0.0140	0.0594	4.3	0.47
8B	0.00374	0.00939	0.0466	3.4	0.40
9B	0.00464	0.0111	0.0472	3.4	0.47
10B	0.00554	0.00728	0.0371	2.7	0.39
11B	0.00644	0.00550	0.0317	2.3	0.35
12B	0.00734	0.00356	0.0268	2.0	0.27

mented with spatial area (or volume) averaging in the plane parallel to the averaged bed surface. This was combined with a decomposition of time-averaged variables into spatially averaged and spatially fluctuating components, which is analogous to the Reynolds decomposition for instantaneous variables. It is then possible to obtain double-averaged (in time and then in space) momentum and mass conservation equations for the flow both above and within the roughness elements of beds.

[6] A number of studies have applied this framework to rough-bed flows [e.g., *Nikora et al.*, 2004; *Campbell et al.*, 2005; *Aberle*, 2006; *Koll*, 2006; *Aberle et al.*, 2007; *Manes et al.*, 2007; *Nikora et al.*, 2007; *Pokrajac et al.*, 2007; *Mignot et al.*, 2009; *Ferreira et al.*, 2010]. Only two experimental studies have made detailed consideration of the number of velocity measurements that are required when applying the spatial averaging framework to their data. *Buffin-Bélanger et al.* [2006] examined how the precision in their estimations of double-averaged streamwise and vertical velocity, and turbulent kinetic energy, changed with the number of velocity measurements over a water-worked gravel bed in a laboratory flume. They discovered that a 10-fold improvement in precision required a 100-fold increase in the number of velocity measurement locations. Also, they found that around two orders of magnitude more locations were required to estimate turbulent kinetic energy for the same level of precision. These values were based on assuming a normal probability distribution for the spatial distribution of the flow parameters. *Aberle et al.* [2008] examined the influence of the number of measurement locations on form-induced stress over static armor layers. They demonstrated that the location of individual point measurements strongly influences the resulting form-induced stress averaged over an area of the bed. They concluded that the number of measurement locations made little difference to the shape of the form-induced stress profiles but contributed significantly to the estimated form-induced stress magnitude. This highlights a need to quantify the number of measurement locations required to produce a spatially averaged quantity which is insensitive to changes in the number or location of measurements. No previous study has provided relationships which allow the prediction of the number of measurement locations needed without a priori information being required about the dynamics of the flow.

[7] This paper describes a series of tests in which flow velocities have been measured in a detailed spatial pattern over two water-worked gravel beds. The data have been used to study the turbulence and spatial flow characteristics for a range of flow submergences. The aim of the paper is to (1) estimate the minimum density of measurements required to provide representative spatially averaged flow parameters over water-worked gravel beds and (2) to assess the influence of the density of measurements on the accuracy of the estimates of these parameters.

2. Methodology

2.1. Experimental Program

[8] The tests were conducted in a tilting, 18.3 m long, 0.5 m wide laboratory flume. Two different sediment mixtures were used and were chosen to characterize the two types of grain-size distributions commonly observed in U.K. gravel-bed rivers: a log-normal, unimodal grain-size distribution and a slightly bimodal grain-size distribution. The former had a grain-size range of 0.15 mm$< D <$ 14 mm and a median grain diameter D_{50} of 4.97 mm. The bimodal mixture was created by adding 25% sand to the unimodal mixture to produce a distribution with the same range of grain sizes and D_{50} of 4.41 mm. The two mixtures were designed to produce similar values of D_{50} so that the average scale of the grains in each of the beds was comparable, but the water-worked surface topography was different.

[9] A total of 24 tests were carried out using a range of bed slopes and relative submergences (Table 1). The selected flow conditions were below those required for bed movement, so the bed surface topography did not change during each test. For each experimental run, a steady flow rate was introduced and the downstream weir was adjusted to achieve uniform depth h for as large a reach as possible. Examination of the flow Reynolds number indicated that all the flows were fully turbulent. The experimental program was designed so that tests with similar values of relative submergence and bed slope were conducted for each bed, so that results could be compared directly between the two sediment beds.

[10] The sediment beds were formed by feeding material into running water, with the feed rate being twice the estimated transport capacity of the flow. In each case, a deposit formed progressively over time. The statistical properties of the two beds are shown in Table 2 and Figure 1a. These show that the surface variation in the second bed containing the sand was less, with lower values of standard deviation and range. The horizontal roughness length scales for this bed are around half the length for the unimodal bed. The surfaces of the two beds were water-worked and armored. Further

Table 2. A Summary of the Bed Surface Properties of the Two Beds, Where σ_b is the Standard Deviation, k is the Range, Sk_b is the Skewness and Ku_b is the Kurtosis of the Distribution of Bed Surface Elevations, and L_x and L_y are the Correlation Lengths (Derived From 2-D Structure Functions) of the Bed Surface Elevations in the Streamwise and Lateral Directions, Respectively

Property	Unimodal bed	Bimodal bed
σ_b (m)	0.00214	0.00170
k (m)	0.0152	0.0137
Sk_b	0.0985	0.0462
Ku_b	2.837	3.015
L_x(m)	0.0135	0.00764
L_y(m)	0.0149	0.00778

information on their bed surface topographies and the way they were formed can be found in *Cooper and Tait* [2009].

2.2. Velocity Measurements

[11] A 2-D Particle Image Velocimetry (PIV) system was used to provide detailed spatial measurements of fluid velocity over the two beds. It was operated at 9 Hz, and the flow was sampled for 5.5 min. Previous approaches to utilize PIV to study rough-bed flows have taken measurements at one lateral position by using a vertical light sheet oriented normal to the bed surface [e.g., *Campbell et al.*, 2005; *Sambrook Smith and Nicholas*, 2005; *Hardy et al.*, 2009]. In this study, PIV measurements were taken in a vertical plane at nine lateral positions across the bed: −88 mm, −66 mm, −44 mm, −22 mm, 0 mm, 22 mm, 44 mm, 66 mm, and 88 mm. A lateral position of 0 mm denotes the center line of the flume. At each lateral position, a streamwise length of 143 mm was imaged and the measurement area was 9.1 m from the flume inlet. This configuration enabled streamwise and vertical velocity to be measured both within the roughness elements and up to the water surface at different streamwise and vertical positions. An interrogation area of 32 × 32 pixels was used in the cross-correlation of the images and corresponded to an area of 4.5 × 4.5 mm. The size of the interrogation area was chosen so that there was little variation in velocity values within an interrogation area, ensuring that the flow can be considered homogeneous within this area. Velocity gradients within an interrogation area can cause outliers and zero-velocity bias. To minimize the problem of bias, an area was chosen so that particle displacements were equal to or less than one fourth of the length of the interrogation area. The interrogation areas were overlapped by 50% in both the streamwise and vertical directions. Overlapping produces more vectors, but this does not equate to an increase in spatial resolution. Instead it can be considered as an oversampling of the flow field. This means that the measurements are not spatially independent and an initial spatial filter (or spatial averaging) has been applied to the data.

[12] The image analysis provided a maximum of 61 velocity measurements in the streamwise direction at each lateral position. Above the roughness elements, the maximum number of measurements available for spatial averaging was therefore 549 at a given measurement height. The separation distance between measurements, in both the streamwise and vertical directions, was 2.25 mm. The spatial resolution of the velocity measurements is equal to the length of the interrogation area. This gives a spatial resolution of 4.50 mm. This means that the PIV measurements were able to resolve large-scale structural features rather than those with dimensions of

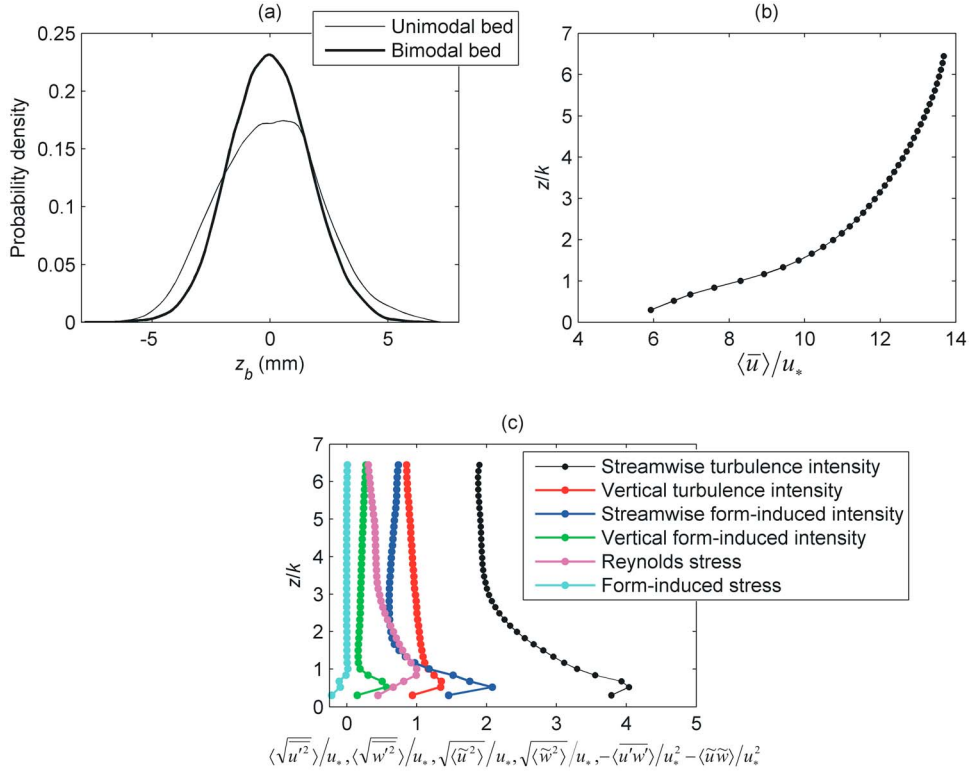

Figure 1. (a) The probability density function of the bed elevations from the zero mean surface elevation z_b for the two beds. (b) and (c) Examples of vertical profiles of spatially averaged flow parameters.

the Taylor's microscale, which is generally the case in PIV. The vertical z-coordinate has the origin at the minimum level of the bed surface. This level was resolved from the detrended laser scans of the bed surfaces and matched to the level within the PIV images, in which the camera was aligned parallel to the average bed slope.

[13] For each experimental run, the instantaneous velocities u were used to derive turbulence and spatial flow characteristics. This was achieved by time-averaging these velocities and applying a Reynolds decomposition. This was supplemented with spatial averaging and a spatial decomposition; see *Nikora et al.* [2001]. The averaging area A_f was planar and parallel to the bed surface. The time-averaged variables were decomposed into spatially averaged and spatially fluctuating components, such that $\overline{u} = \langle \overline{u} \rangle + \tilde{u}$. The angled brackets denote that the variable is spatially averaged. The spatial fluctuations arise from the difference between the double-averaged $\langle \overline{u} \rangle$ and time-averaged $\overline{u}$ values, similar to the conventional Reynolds decomposition of $u' = u - \overline{u}$. Thus, by combining time and spatial averaging approaches, it was possible to derive the double-averaged characteristics of the flow, such that both the temporal and spatial variability in the flow is explicitly taken into account. The analysis concentrates on examining the double-averaged streamwise velocity $\langle \overline{u} \rangle$, spatially averaged turbulence intensities $\langle \sqrt{\overline{u'^2}} \rangle$ and $\langle \sqrt{\overline{w'^2}} \rangle$, form-induced intensities $\sqrt{\langle \tilde{u}^2 \rangle}$ and $\sqrt{\langle \tilde{w}^2 \rangle}$, spatially averaged Reynolds stress $\langle \overline{u'w'} \rangle$ and form-induced stress $\langle \tilde{u}\tilde{w} \rangle$. An example of the vertical profiles of these parameters is shown in Figure 1. Further profiles can be found in *Cooper and Tait* [2010].

[14] A previous study by the authors made a comparison between the spatially averaged flow variables estimated from 20 Laser Doppler Anemometry (LDA) profiles and from 168 PIV profiles [*Koll et al.*, 2008]. This was done to understand how a difference in size of sampling volume (interrogation area/control volume), sampling rate, measurement principles, and number of profiles influenced these estimates. It was discovered that the shape of the vertical profiles of time-averaged streamwise velocity showed a good agreement between LDA and PIV, although systematic deviations in the absolute values were evident. Larger deviations were observed between the time-averaged vertical velocities. An investigation of the spatially averaged turbulent flow properties revealed major differences in vertical turbulence intensities but closer agreement in streamwise turbulence intensities. There was also a considerable difference in Reynolds stress. This was not attributable to the number of profiles, because there was little difference in the values between 20 and 168 PIV profiles. It was concluded that the deviation in values between PIV and LDA may have occurred because of a difference in sampling rate or the size of the sampling volume. It was not possible to determine which effect was most dominant above the roughness elements. The sampling rate was comparable for the two measurement systems within the elements, suggesting that a difference in the size of the sampling volume was the contributing factor. The results found by *Koll et al.* [2008] suggest that our PIV measurements may overestimate streamwise turbulence intensity and underestimate vertical turbulence intensity and spatially averaged Reynolds stress.

2.3. Spatially Representative Flow Measurements

[15] Two previous studies examining the representativeness of flow measurements over gravel beds have discussed the influence of the number of measurement locations [*Buffin-Bélanger et al.*, 2006; *Aberle et al.*, 2008]. A different approach is used here. Estimation is made of the minimum measurement density, defined as the ratio of the minimum number of measurements $N_{\min}$ to the averaging area A_f needed to obtain flow parameter estimations with a known level of precision and accuracy. The total possible averaging area A_0 is equal to 143 × 176 mm^2 (streamwise × lateral), which is the planar area covered by the PIV measurements and includes all the measurement locations (highest measurement density). The streamwise length is given by the length of the PIV image, and the lateral dimension is equal to the lateral span covered by the nine PIV planes. Within the roughness elements, this averaging area A_0 is intersected by surface grains, so it reduces from the roughness crest to the roughness trough. To allow for this reduction, the fluid averaging area A_f is set to be equal to A/A_0, where A is the roughness geometry function, which is defined as A_f / A_0 and resolved from a laser scan of the bed. This allows the density to be assessed within the roughness elements, accounts for the reduction in measurement locations down to the trough and eliminates any influence of this reduction on the level of representation of the measurements. *Aberle* [2007] showed that the estimation of A using a laser displacement sensor is valid for the upper 70% of the layer within the roughness elements. The PIV measurements only cover this proportion, so A can be used to calculate A_f. The minimum density $N_{\min} / A_f$ is scaled by the bed streamwise correlation length scale L_x (derived from a 2-D structure function; *Nikora et al.*, 1998) and flow length scale ν/u_* to give $N_{\min} L_x^2 / A_f$ and $N_{\min} (\nu/u_*)^2 / A_f$, where ν is the kinematic viscosity of water and u_* is bed shear velocity. This allows the influence of the scaling of bed roughness and flow properties on minimum density to be explored. The two dimensionless measures are from here on collectively referred to as "minimum density," and the notations D_b and D_f are used, respectively. The maximum D_b for the unimodal and bimodal beds are 2.8 and 1.3, respectively, and the maximum D_f values range from 3896 to 60,012, according to flow conditions. The shear velocity is defined by $u_* = \sqrt{\tau_0/\rho}$ where τ_0 is the total fluid stress at the roughness crest, as suggested by *Manes et al.* [2007]. The total fluid stress was estimated by linearly extrapolating the spatially averaged Reynolds stress from the layer above the bed surface down to the roughness crest. *Manes et al.* [2007] argued that the shear velocity at the roughness crest rather than the roughness trough is the most appropriate scaling parameter when dealing with flows with a range of relative submergences.

[16] To evaluate the minimum measurement density, the values of various spatially averaged parameters were calculated for different measurement densities. In PIV, because the measurements are made within a regular grid, with a small measurement separation distance and the interrogation windows are overlapped, the calculation of a spatially averaged parameter is influenced by correlative effects in the velocity measurements. Neighboring locations are influenced by each other owing to spatial coherence in the flow. To eliminate this influence, at each of these densities the data values were randomly selected from within the area A_f and averaged. If

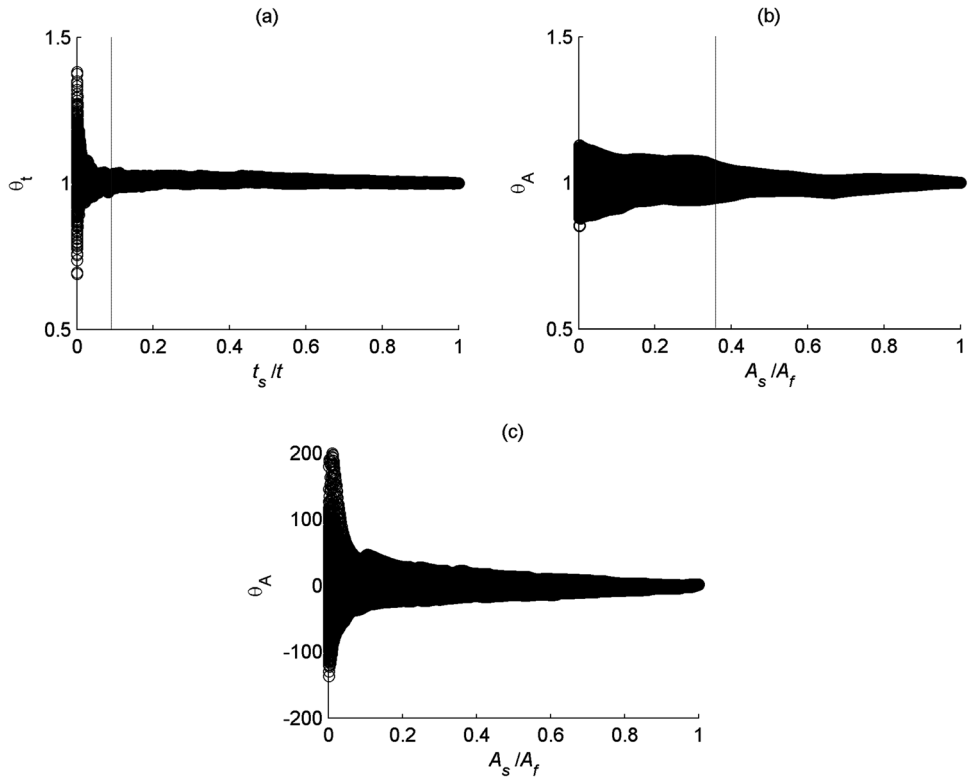

Figure 2. An example of the change in (a) the ratio θ_t of the time-averaged streamwise velocity at averaging time period t_s to that averaged over the total sampling period t. (b) The ratio θ_A of the double-averaged streamwise velocity at averaging area A_s to that averaged over the total area A_f. The vertical line within the plots defines the minimum required sampling time and averaging area. This is shown for experimental run 6U at $z/k = 1.01$. Plot (a) is taken from measurements on the centreline of the flume, and for plots (b) and (c) the averaging is carried out from the point measurement scale to the total area covered by all the measurements. Note the larger scale on the vertical axis in (c). The θ_A values are particularly high (and low) because the form-induced stress is very small at this height (see Figure 1c).

this was carried out only once for each measurement density, then the estimate of minimum measurement density would be dependent on which measurement locations were randomly selected. To reduce this likelihood, the random sampling was repeated 100 times. Therefore, the values associated with each density are obtained from 100 spatially averaged values. The minimum measurement density was estimated to be the density at which 95% of these 100 repetitions fell within 5% of the averaged parameter value obtained using all the measurements. The 95% represents the level of precision, and the 5% is the accepted level of inaccuracy. A difference of less than 5% in the parameter at the minimum density was deemed appropriate because a significance level of 5% is most often used to assess significant statistical differences between variables. If the number of samples was less than 100, the same procedure was used and some locations were sampled more than once.

[17] To ensure that the sampling time and sampling area were sufficient to provide temporally and spatially representative estimates of the flow parameters, an examination was made into how the flow parameters changed in time and space. An example is shown in Figure 2a for experimental run 6U of how the time-averaged streamwise velocity at each measurement location on the center line of the flume varied during different averaging time periods at $z/k = 1.01$, i.e., close to the top of the roughness elements. The minimum sampling period required to provide a temporally representative value was estimated in a similar manner to the minimum density. It was considered to be the averaging period at which 95% of the time-averaged values fell within 5% of the parameter averaged over the total sampling time. This condition is illustrated in Figure 2a. It shows that the sampling time used was clearly long enough to provide temporally representative values of time-averaged streamwise velocity. This was found to be the case for all other hydraulic parameters and experimental runs used in this study.

[18] The minimum averaging area was defined in a similar manner. For each measurement location, the hydraulic parameters were averaged over every possible averaging area within the total available averaging area A_f. An example is shown in Figure 2b for the same experimental run for the double-averaged streamwise velocity. The averaging was carried out from the point measurement scale to the total area covered by all the measurements. The minimum averaging area was estimated to be the area at which 95% of the spatially averaged values fell within 5% of the parameter averaged over the whole bed. The results reveal that for these conditions, the averaging area A_f was larger than the minimum required to provide representative values of double-averaged streamwise velocity. The velocity estimates become fairly insensitive with changes in averaging area close to A_f. This type of analysis was undertaken for all other hydraulic

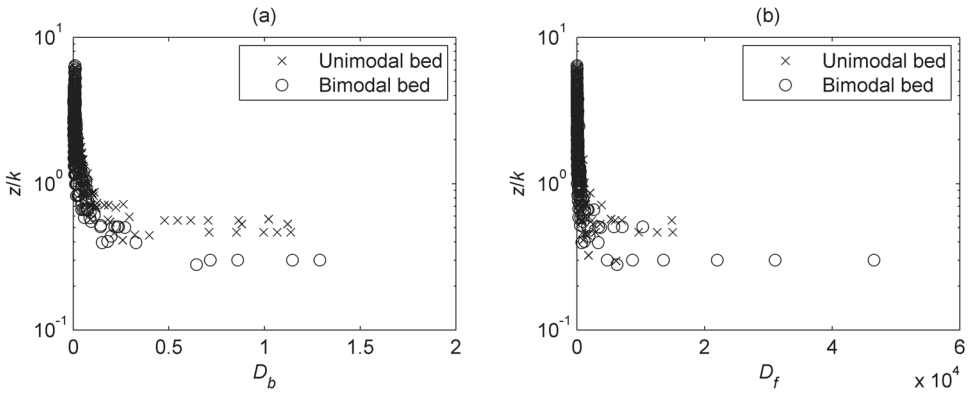

Figure 3. Vertical profiles of the minimum density of measurements, defined by (a) D_b and (b) D_f, to produce representative values of $\langle \overline{u} \rangle$ for all 24 experimental runs.

parameters and experimental runs. It was found that A_f was larger than the required minimum for all flow parameters at the stated precision and accuracy levels, and the averages were stable, except for form-induced stress (Figure 2c). In the latter case, this condition was only met for some measurement heights. It is therefore not possible to determine whether the maximum averaging area was sufficient for estimating form-induced stress. Strictly speaking, this means that the averaging area was not large enough to determine accurately form-induced stress. This indicates that the spatial averaging area was large enough to capture the flow spatial variability at the scale of the grains, but a larger area was required for the flow to be considered spatially uniform. For the analysis of the minimum required measurement density, we make the assumption that the form-induced stress derived from all the measurements at the largest averaging area is the unbiased value.

3. Results

3.1. Minimum Measurement Density

[19] The variation in the minimum density of measurements required to provide a representative value of $\langle \overline{u} \rangle$ is shown in Figure 3. This is shown for both D_b and D_f for all 24 experimental runs over the two beds. It displays the variation in minimum measurement density with z/k, where k is given by the range in bed surface elevations (geometric roughness height). Figure 3 reveals that there is a small variation in density at a given z/k between the different hydraulic conditions for the flow above the two beds. Also, the density is slightly better scaled by the flow length scale. The required minimum density is low within the flow above the bed and then increases slightly toward the roughness crest ($z/k = 1$). There is a rapid increase in density below the roughness crest, where the largest values of measurement density are observed. The largest values indicate that the required density near to the roughness troughs is close to the maximum measurement density collected in this study. The minimum density, when scaled by a flow length scale, is largely independent of the hydraulic conditions and the properties of the bed surface, but is highly dependent on z/k above the bed surface. Empirical relationships for D_f can be derived using best-fit equations. Within the roughness elements, the curve of D_f for the two beds can be described by a single power relationship with z/k. Above the bed, where the vertical profiles adopt a different shape, a best fit is made by another form of a power relationship with z/k. Table 3 lists the two best-fit functions for these data.

[20] Figure 4 shows that for $\langle \sqrt{\overline{u'^2}} \rangle$ and $\langle \sqrt{\overline{w'^2}} \rangle$ the variation in minimum density between the two beds is again slightly reduced when scaled by a flow length scale. This was found to be much clearer for the form-induced intensities and

Table 3. Fitted Relationships for Estimating the Minimum Density of Measurements Required to Produce a Representative Value of Each of the Spatially Averaged Flow Parameters[a]

Parameter	Relationship	Condition
$\langle \overline{u} \rangle$	$D_f = 266(z/k)^{-2.90}$	$z/k \le 1$
	$D_f = 232(z/k)^{-1.51}$	$z/k > 1$
$\langle \sqrt{\overline{u'^2}} \rangle$	$D_f = a(z/k)^b$	$z/k \le 1$
	where $a = -573(h/k) + 3789$	
	$b = -0.210(h/k) - 1.53$	
	$D_f = c(z/k)^d$	$z/k > 1$
	where $c = -827(h/k) + 5166$	
	$d = 0.224(h/k) - 0.803$	
$\langle \sqrt{\overline{w'^2}} \rangle$	$D_f = a(z/k)^b$	$z/k \le 1$
	where $a = -839(h/k) + 5518$	
	$b = -0.272(h/k) - 1.32$	
	$D_f = c(z/k)^d$	$z/k > 1$
	where $c = -1291(h/k) + 8149$	
	$d = 0.120(h/k) - 1.28$	
$\sqrt{\langle \tilde{u}^2 \rangle}$	$D_f = a(z/k)^b$	$z/k \le 1$
	where $a = -2333(h/k) + 18737$	
	$b = 0.0844(h/k) - 1.18$	
	$D_f = c(z/k)^d$	$z/k > 1$
	where $c = -1994(h/k) + 14987$	
	$d = -0.0843(h/k) - 0.496$	
$\sqrt{\langle \tilde{w}^2 \rangle}$	$D_f = a(z/k)^b$	$z/k \le 1$
	where $a = -4836(h/k) + 35037$	
	$b = 0.0358(h/k) - 0.488$	
	$D_f = c(z/k)^d$	$z/k > 1$
	where $c = -3722(h/k) + 26324$	
	$d = 0.0273(h/k) - 0.254$	
$\langle \overline{u'w'} \rangle$	$D_f = a(z/k) + b$	$z/k \le 1$
	where $a = 8652(h/k) - 61713$	
	$b = -9826(h/k) + 70386$	
	$D_f = c(z/k)^d$	$z/k > 1$
	where $c = -2358(h/k) + 14661$	
	$d = 0.0385(h/k) + 0.387$	

[a]These are fitted from the data for all experimental runs for the two beds, and apply for the range of relative submergences studied ($h/k = 1.2 - 6.2$). The equations are valid for a 95% confidence that the flow parameter estimate will be within 5% of the true spatial mean.

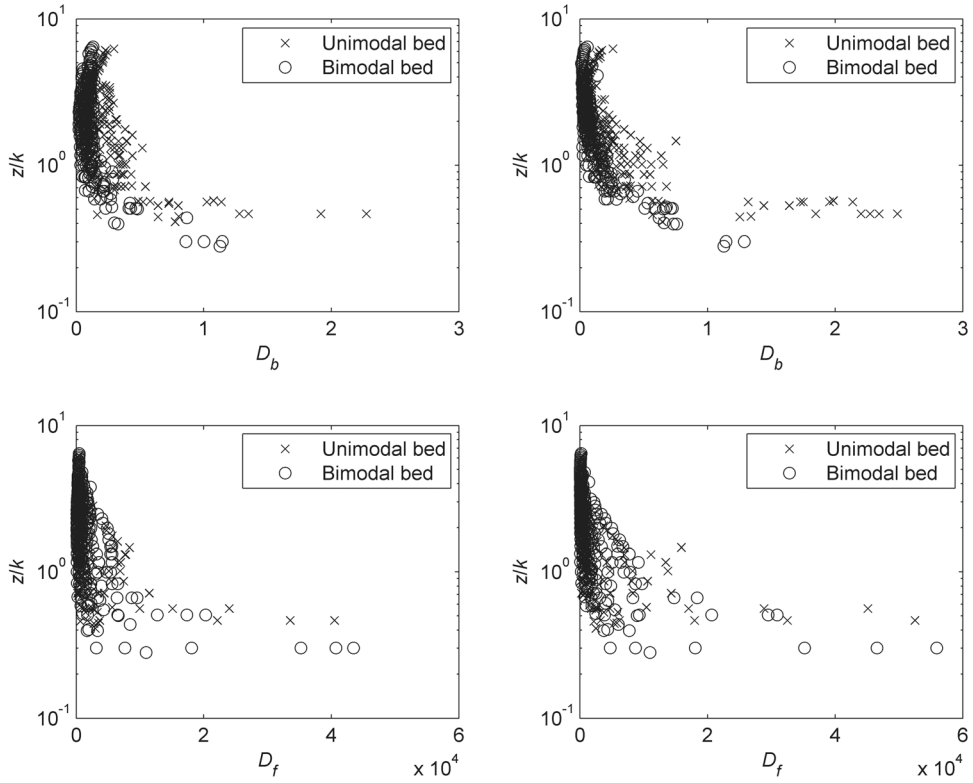

Figure 4. Vertical profiles of the minimum density of measurements to produce representative values of $\langle\sqrt{\overline{u'^2}}\rangle$ (left-hand side) and $\langle\sqrt{\overline{w'^2}}\rangle$ (right-hand side) for all 24 experimental runs.

$\langle\overline{u'w'}\rangle$. The values of D_f for the turbulence intensities are typically larger than for $\langle\overline{u}\rangle$ at all values of z/k. This is plausible, given that $\sqrt{\overline{u'^2}}$ and $\sqrt{\overline{w'^2}}$ are second-order statistical moments. Unlike Figure 3, there is greater variability in density across the range of hydraulic conditions, although there is still little evidence of systematic difference between the two beds. On closer inspection, the values of D_f for these two parameters, at similar values of z/k, decease with a rise in relative submergence h/k. Figure 5 shows that this trend is common across both beds. This confirms the expectation that deeper flows require a lower measurement density because there is less spatial variability in turbulence.

Within the roughness elements, the individual profiles for $\langle\sqrt{\overline{u'^2}}\rangle$ and $\langle\sqrt{\overline{w'^2}}\rangle$ are described by a power relationship with z/k for both beds, and its parameters are dependent upon relative submergence (Table 3). Figures 6a and 6b show that the parameter a for this power relationship for both turbulent intensities displays a decrease with submergence, but exponent b has only a very slight correlation and greater variability in its values between the two beds. Above the bed surface, the profiles of D_f can also be described by another power relationship with z/k. The parameter c for this relationship for both turbulence intensities varies in a similar manner with submergence (Figures 6c and 6d), as was seen for a, but not as consistently. The exponent d tends to slightly increase with a rise in submergence. The individual changes in the parameters a, b, c, d in Figure 6 are consistent across both beds, showing that a single equation for each of the four parameters can be used for both beds.

[21] Close to the roughness troughs, the maximum measurement density is required to provide representative values of $\sqrt{\langle\tilde{u}^2\rangle}$ and $\sqrt{\langle\tilde{w}^2\rangle}$ for all the experimental conditions (Figure 7), indicating tests in which the PIV measurement density was insufficient. The minimum required measurement density is higher than for the other flow parameters because $\sqrt{\langle\tilde{u}^2\rangle}$ and $\sqrt{\langle\tilde{w}^2\rangle}$ are higher order moments than the previously analyzed flow variables. The minimum density values for $\sqrt{\langle\tilde{u}^2\rangle}$ and $\sqrt{\langle\tilde{w}^2\rangle}$ display much greater variation between the different hydraulic conditions than seen for the other flow variables. Figure 7 shows that this is largely due to the minimum density decreasing with a rise in relative submergence. This again conforms to the expectation that flows with a higher submergence (deeper flows) require a lower measurement density because there are likely to be lower levels of spatial variability in the time-averaged flow. Table 3 shows that D_f is again well described by a power relationship with z/k for the flow both above and within the roughness elements. Figure 8 confirms that the parameters for the best-fit functions also vary in a largely similar manner with relative submergence as was observed for the turbulence intensities.

[22] The values of D_f for $\langle\overline{u'w'}\rangle$ are very similar to those seen for these intensities and vary in the same manner with relative submergence (Figure 9). They can be described by a linear function within the roughness elements and a power

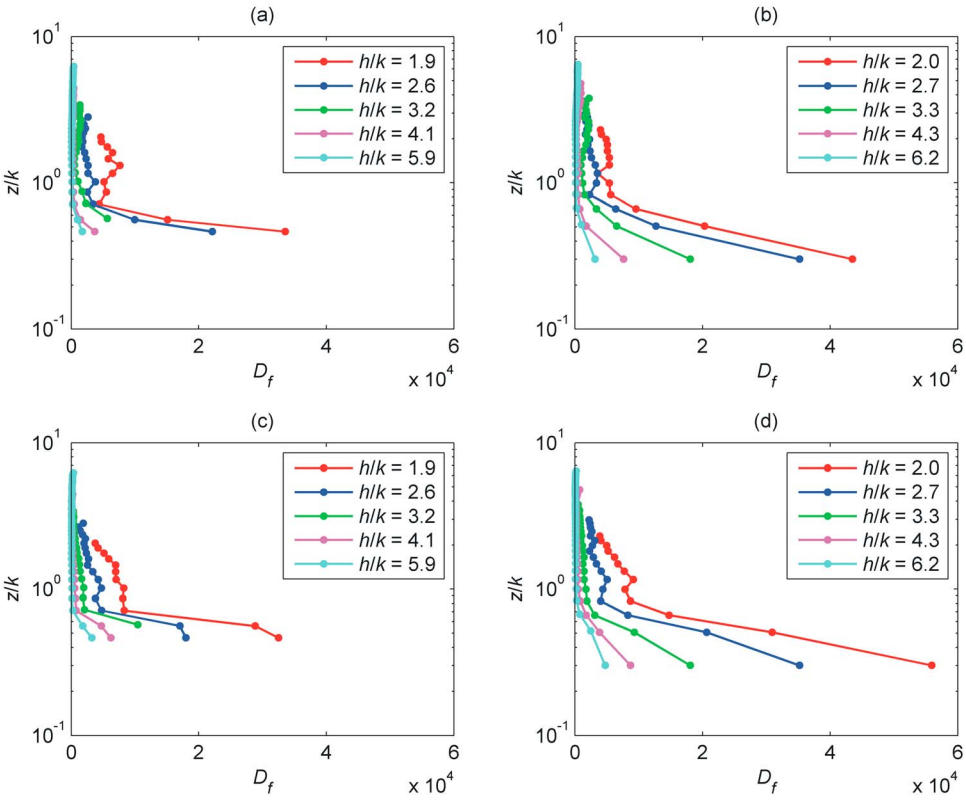

Figure 5. The change in the vertical profiles of the minimum density of measurements to produce representative values of $\langle\sqrt{\overline{u'^2}}\rangle$ with relative submergence for (a) the unimodal bed and (b) the bimodal bed; and of $\langle\sqrt{\overline{w'^2}}\rangle$ for (c) the unimodal bed and (d) the bimodal bed. This is shown for a selection of the experimental runs.

relationship above (Table 3). The results for $\langle\tilde{u}\tilde{w}\rangle$ are different. The maximum measurement density is required to provide values of $\langle\tilde{u}\tilde{w}\rangle$ at the same accuracy as the other flow variables, revealing that the sampling density was not sufficient. To assess the accuracy of estimating $\langle\tilde{u}\tilde{w}\rangle$ using the available velocity measurements at the 95% level of precision, we need to make the assumption that the form-induced stress derived at the maximum measurement density is the unbiased value for the bed. On the basis of this assumption, the best level of accuracy that can be achieved is 50–60%. This is when the required density is lower than the maximum density for all of the flow depth.

3.2. Implications of Sampling at a Different Density

[23] To gain an understanding of the implications of sampling at a lower measurement density than D_f, the raw values used for estimating the minimum density are again examined. Figure 10 displays the results from all 24 experimental runs and shows how the percentage error in the estimate of each of the flow parameters changes with measurement density. For each measurement density, a spatially averaged value was derived and compared to that produced using all the measurements (maximum density). This was repeated 100 times at each measurement density so that there were 100 spatially averaged values per density. The percentage error was estimated to be the level of error at which 95% of these 100 values fell. This was carried out using measurements at the lowest height within the roughness elements (z/k = 0.47) and close to the roughness crest (z/k = 1.01). Therefore, Figure 10 represents the highest likely errors for the roughness elements and for the flow above the bed surface. The plots show how the errors progressively change with measurement density and provide a clear indication of the importance of choosing the correct density. This is useful because when bed and flow conditions are similar, it indicates whether the spatially averaged values estimated by studies using different measurement densities are comparable.

[24] The results reveal that at densities just lower than the required minimum density in Figure 3, there is typically up to a 30% error in the estimation of $\langle\overline{u}\rangle$, both within the roughness elements and above the bed surface. At the roughness crest, this error level quickly reduces with a rise in measurement density. Beyond a density of around 1000 (higher than the required minimum), the level of error is fairly insensitive to changes in measurement density, falling to up to 2%. Within the roughness elements, the percentage error is more sensitive to changes in measurement density.

[25] Similar results can be seen for $\langle\sqrt{\overline{u'^2}}\rangle$ and $\langle\sqrt{\overline{w'^2}}\rangle$ (Figures 10b and 10c), although the errors are slightly higher. At the lowest densities, they can be typically up to 60%, both above the bed surface and within the roughness elements. At densities just lower than D_f of between 1000 and 30,000, they can be up to between 18 to 60% within the roughness

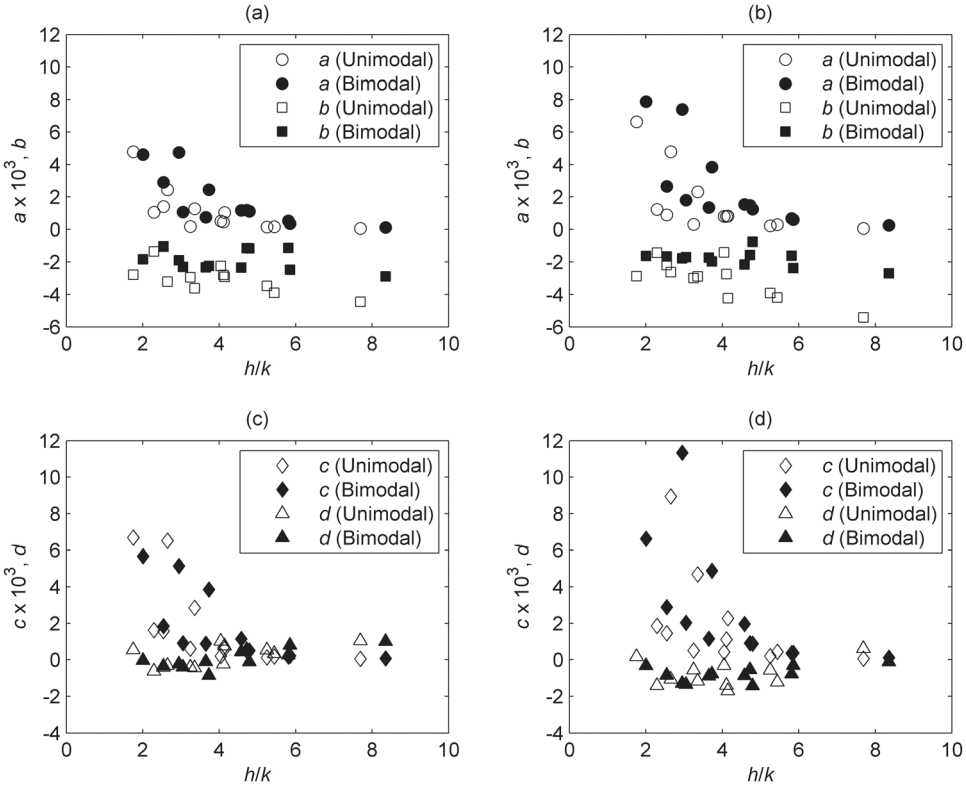

Figure 6. The change in the parameters a and b in the fitted relationships for $z/k \leq 1$ of (a) $\langle\sqrt{\overline{u'^2}}\rangle$ and (b) $\langle\sqrt{\overline{w'^2}}\rangle$; and parameters c and d in the fitted relationships for $z/k > 1$ of (c) $\langle\sqrt{\overline{u'^2}}\rangle$ and (d) $\langle\sqrt{\overline{w'^2}}\rangle$.

elements. Above the bed surface, for densities below D_f (up to 8000), the errors are typically up to between 5 and 60%, owing to a large change in percentage error with measurement density.

[26] The errors are higher for the estimation of the form-induced intensities, particularly $\sqrt{\langle\tilde{w}^2\rangle}$ (Figures 10d and 10e). At the lowest measurement densities, the error levels can typically be up to 150 and 200% for $\sqrt{\langle\tilde{u}^2\rangle}$ and $\sqrt{\langle\tilde{w}^2\rangle}$, respectively. Within the roughness elements, at densities which are just lower than D_f of between 2000 and 40,000, these are still considerable; typically up to around 200% and 25%, respectively. For the flow above the bed and at densities of between 1000 and 30,000 (which are just below the required minimum) the errors typically range from 20 to 150%. The error levels also vary greatly with changes in measurement density, revealing that the estimation of form-induced intensity is highly sensitive to the measurement density used.

[27] Figure 10f shows that the errors in the estimation of $\langle\overline{u'w'}\rangle$ within the roughness elements are considerably higher. Within the roughness elements, the error level can be typically up to 400% at the lower measurement densities. Closer to D_f, at densities of between 4000 and 40,000, this reduces to up to 30–150%. These larger errors are observed because the fluid area within this layer is much smaller than above the bed. This means that the estimation of $\langle\overline{u'w'}\rangle$ is very sensitive to the measurement density which is used. A large proportion of the stress can be transferred by a small number of locations, and the spatial variability in stress is therefore higher. Above the bed surface, the errors are up to 100% at the lowest densities and then quickly reduce with a rise in measurement density. They obtain a maximum value above 1200 of around 20%, which corresponds to the error level for measurements at densities just lower than D_f.

4. Discussion

4.1. Scaling of Minimum Measurement Density

[28] The minimum required measurement density for all of the spatially averaged flow parameters was dependent on measurement height, with the values increasing significantly within the roughness elements. The profile shape was similar for each of the flow variables, but the minimum density differed. For a particular spatially averaged parameter, the vertical profile shape and the minimum measurement density at a given height were reasonably consistent for the two beds at a similar level of relative submergence. For all but the double-averaged streamwise velocity, the minimum density at a given height decreased with a rise in relative submergence, and it reduced more quickly with height for shallower flows. This was consistent for the two beds and occurred for both the flow within and above the roughness elements.

[29] The difference in the minimum required measurement density was smaller when scaled by a flow length scale rather than streamwise bed roughness length scale. This reveals that the minimum density at a given height is more sensitive to the spatial structure of the flow than the bed. Given that the density was not equally well scaled by these two length scales

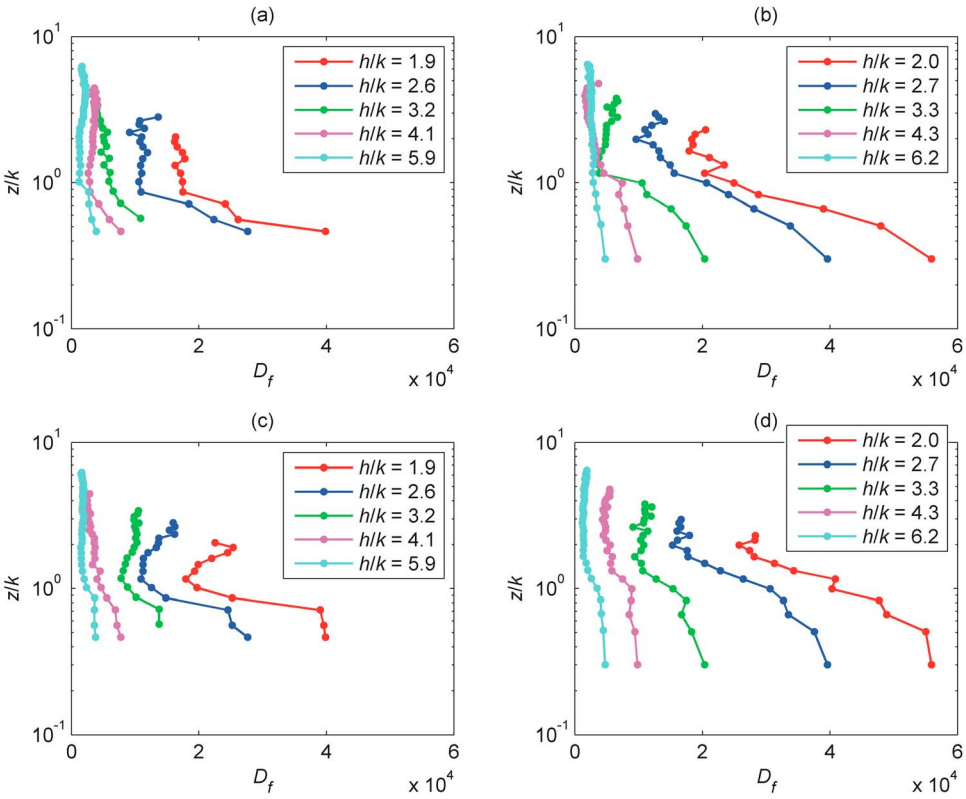

Figure 7. The change in the vertical profiles of the minimum density of measurements to produce representative values of $\sqrt{\langle \tilde{u}^2 \rangle}$ with relative submergence for (a) the unimodal bed and (b) the bimodal bed; and of $\sqrt{\langle \tilde{w}^2 \rangle}$ for (c) the unimodal bed and (d) the bimodal bed. This is shown for a selection of the experimental runs.

for all of the flow variables, it implies that the flow length scale (and structure) is also not well scaled by the bed roughness length scale. This agrees with the laboratory observations of *Cooper and Tait* [2008], who over the same two gravel beds observed that the spatial organization of the time-averaged flow is not well associated with the bed surface topography. It also supports the findings of *Lamarre and Roy* [2005] and *Legleiter et al.* [2007], who carried out velocity measurements in gravel-bed rivers at the reach scale. *Lamarre and Roy* [2005] found that roughness elements had surprisingly little impact on the spatial organization of the flow at the reach scale, despite a topographically complex channel boundary. They observed that the complexity of the bed was not reflected in the spatial variability of vertical profiles of time-averaged streamwise velocity. As a result, they concluded that the distribution of the mean flow properties displayed a well-organized, coherent spatial pattern that was controlled by flow depth rather than by abrupt, isolated changes associated with individual clasts. *Legleiter et al.* [2007] also discovered results which supported these claims, even in flows where the flow depth was of the same order as the D_{84} of the bed. Individual roughness elements were found to have little correlation with the flow, and flow depth had a fundamental control over spatial flow structure.

4.2. Application of Results

[30] Empirical relationships have been presented which relate minimum measurement density to relative height for a number of spatially averaged flow parameters. These are based on measurements across a range of hydraulic conditions and over beds with different surface topographies. These two beds can be classed as macroscopically flat, exhibiting no significant, large bed forms, no large isolated roughness elements, and a relatively low (to field conditions) grain-size range. The beds are water-worked, armored, well imbricated, and have a preferential alignment of grains and small-scale bed features in the streamwise direction, as reflected in the horizontal roughness length scales. The similarity in the scaling with measurement height, flow length scale, and relative submergence for the two beds further suggest that it is reasonable to use the empirical relationships to predict the required minimum measurement density for similar macroscopically flat beds. Strictly, these are only valid for the range of relative submergences studied here ($h/k = 1.2 - 6.2$), but it is likely that they could also be used for flows with larger submergences, but not those which are lower.

[31] It is doubtful that the empirical relationships will be relevant to beds which are not macroscopically flat and to those which exhibit significant, large bedforms and large isolated roughness elements. To provide some indication of how the measurement densities differ between studies, Table 4 lists the estimated values of N, A_f and $N(v/u_*)^2 / A_f$ for those with a similar range of relative submergences. It shows that the density achieved by point velocity measurements is two to seven orders of magnitude lower than that achieved by

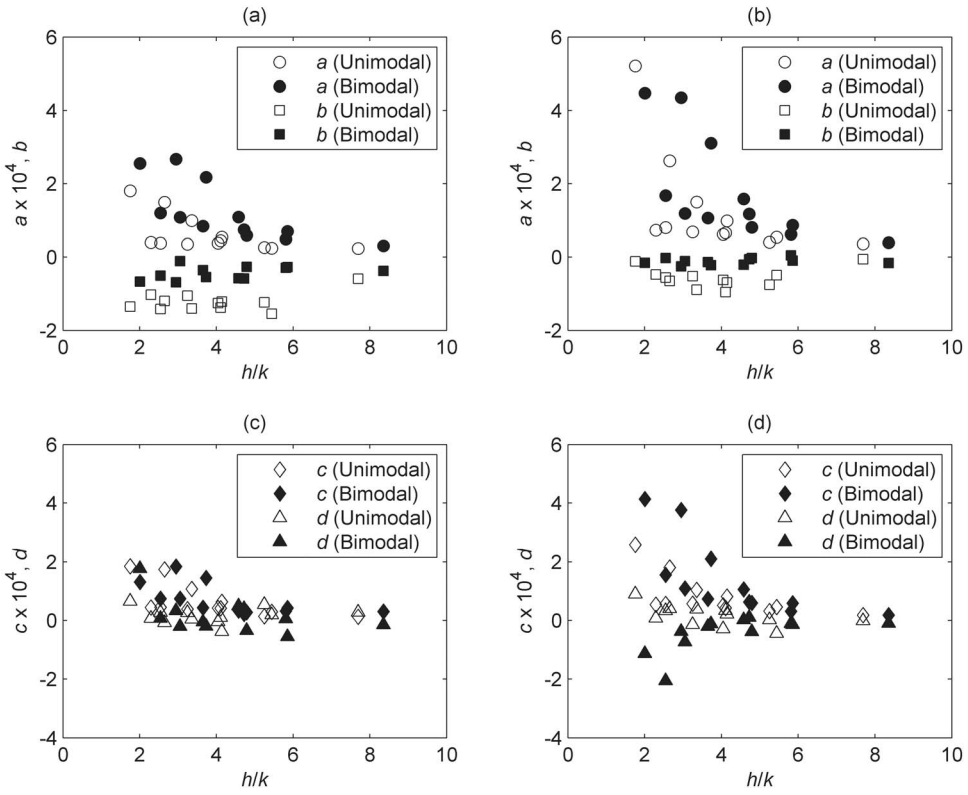

Figure 8. The change in the parameters a and b in the fitted relationships for $z/k \leq 1$ of (a) $\sqrt{\langle \tilde{u}^2 \rangle}$ and (b) $\sqrt{\langle \tilde{w}^2 \rangle}$; and parameters c and d in the fitted relationships for $z/k > 1$ of (c) $\sqrt{\langle \tilde{u}^2 \rangle}$ and (d) $\sqrt{\langle \tilde{w}^2 \rangle}$.

PIV studies. If the influence of measurement density on the level of error in the estimation of the flow parameters were similar to that seen in Figure 10, it would clearly show that the potential errors in using point velocity measurements at these kinds of densities would be significant.

4.3. Implications for Performing Velocity Measurements

[32] The results show that a relatively low density of velocity measurements is required to represent accurately double-averaged streamwise velocity above the roughness elements, but the value is an order of magnitude higher within. It is most difficult to make velocity measurements for the flow within the roughness elements. The density of measurements which can be achieved with any velocimeter within this region is dependent on bed geometry, so the need for a high density within the roughness elements represents a key challenge for obtaining accurate measurements of spatially averaged flow parameters.

[33] The density of measurements required for the turbulence intensities was double that for the double-averaged streamwise velocity. The level of errors in estimating the

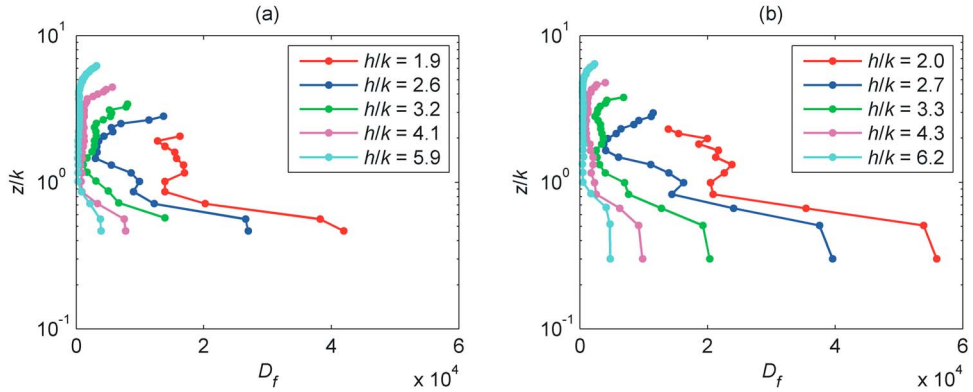

Figure 9. The change in the vertical profiles of the minimum density of measurements to produce representative values of $\langle \overline{u'w'} \rangle$ with relative submergence for (a) the unimodal bed; and (b) the bimodal bed. This is shown for a selection of the experimental runs.

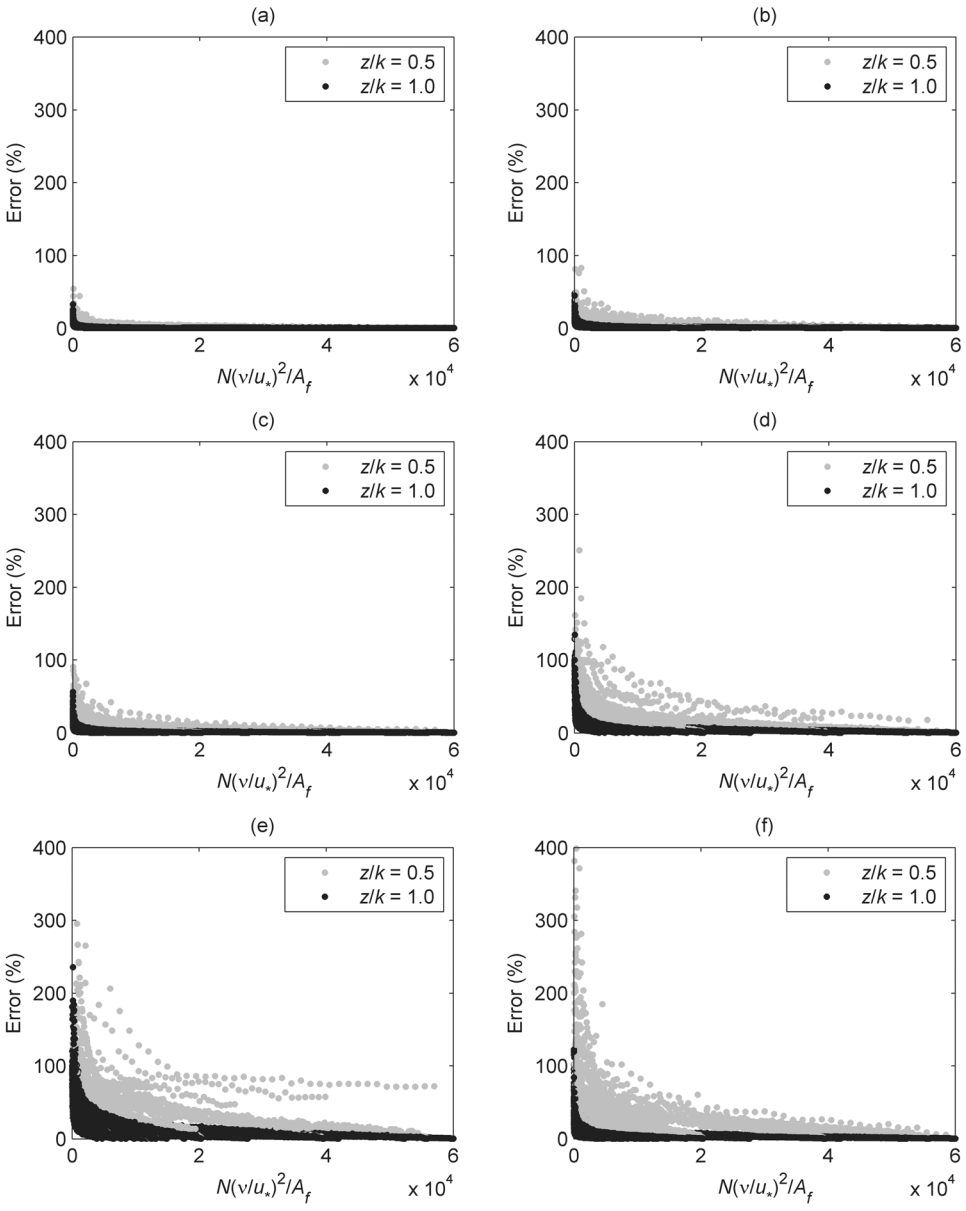

Figure 10. Change in percentage error with measurement density for (a) $\langle \overline{u} \rangle$; (b) $\langle \sqrt{\overline{u'^2}} \rangle$; (c) $\langle \sqrt{\overline{w'^2}} \rangle$; (d) $\sqrt{\langle \tilde{u}^2 \rangle}$; (e) $\sqrt{\langle \tilde{w}^2 \rangle}$; and (f) $\langle \overline{u'w'} \rangle$ for all 24 experimental runs.

Table 4. Summary of the Sampling Routines Performed by a Selection of Previous Studies Over Gravel Beds[a]

Study	N	A_f(m^2)	$N(\nu/u_*)^2/A_f$	h/k
This study	22–549	0.001–0.025	3896–60012	1–6
Lawless and Robert [2001][b,c] plane bed	15	0.6 × 1.6	7.4–35	3–6
Lamarre and Roy [2005][b,c]	25	8.3 × 19.4	0.0055	5
	40	10.0 × 10.4	0.0033	6
Sambrook Smith and Nicholas [2005][d,e]	310	0.001 × 1.0	114188–196872	4
Buffin-Bélanger et al. [2006][c,d]	99	0.5 × 0.8	11	6[f]
Aberle et al. [2008][c,d,g]	12–48	0.6–0.4 × 2.4	0.36–4.9	2–5

[a]The values of A_f are taken to be the planar area of the bed which the velocity measurements cover and are trying to represent.
[b]Field study.
[c]Point velocity measurements.
[d]Laboratory study.
[e]PIV measurements.
[f]Lower studied flow.
[g]Includes *Aberle* [2006], *Aberle et al.* [2007], and *Nikora et al.* [2007].

intensities at lower densities than the required minimum were also a similar magnitude larger. The implications of sampling at a lower density are therefore more considerable. This supports the findings of *Buffin-Bélanger et al.* [2006] for a different turbulence parameter. They observed that the imprecision in the estimation of turbulent kinetic energy was much higher than for the estimation of double-averaged streamwise velocity. They also discovered that imprecision in the two parameters increased with Reynolds number. This was linked to an increase in spatial heterogeneity in time-averaged velocities and turbulence intensities with Reynolds number. These trends contradict our findings. The minimum measurement density for the double-averaged streamwise velocity was not related to relative submergence (and therefore Reynolds number), and the measurement density for the turbulence intensities decreased with an increase in relative submergence. This indicates that the spatial heterogeneity in the turbulence intensities was lower at the higher levels of relative submergence, which appears logical, given the dependence of turbulence intensity on relative roughness. This contradiction can be explained by the difference in flow conditions studied by *Buffin-Bélanger et al.* [2006]. A number of studies have shown that the flow can be considered two-dimensional if the width to flow depth ratio is greater than 3.5 [*Song et al.*, 1994] or greater than 5 [*Nezu and Nakagawa*, 1993; *Kironoto and Graf*, 1994]. The experimental runs carried out by *Buffin-Bélanger et al.* [2006] had ratio values of between 1.6 and 2.4. Hence, the level of spatial heterogeneity in *Buffin-Bélanger et al.* [2006] is likely to be influenced by three-dimensional flow effects and is not directly comparable to the two-dimensional flow considered in our study.

[34] The minimum densities for the form-induced intensities and spatially averaged Reynolds stress were similar. They were higher than for the turbulence intensities, particularly above the roughness elements, in which they could be two times higher. The error levels were also around 50% higher at similar measurement densities. The results revealed that if measurements are made at densities lower than the minimum required density, the likely result is very large under- and overestimation in form-induced intensity and spatially averaged Reynolds stress. These errors are more likely for these parameters because of the higher required minimum measurement density. Any significant errors in the estimation of Reynolds stress is likely to have important implications for the accurate estimation of bed shear stress and bed shear velocity.

[35] At almost all measurement heights, the maximum measurement density provided by the PIV measurements was required to estimate form-induced stress. This is despite the measurements providing a high density of velocity measurements (relative to those studies using point velocity measurements). These results strongly support the findings of *Aberle et al.* [2008]. They concluded that, although the number of measurement locations does not greatly influence the shape of the form-induced stress profile, the magnitude cannot unambiguously be determined from a low density of measurements. *Cooper*'s [2006] results suggest that this is likely to be caused by the high level of spatial variability in correlations between $\tilde{u}_{x,y}$ and $\tilde{w}_{x,y}$, in which particular locations have a significant influence on the absolute values of the mean distribution. *Cooper* [2006] discovered that $\tilde{u}\tilde{w}_{x,y}$ values at some locations over the bed could be as much as double those at other locations. In the majority of cases, the standard deviation in $\tilde{u}\tilde{w}_{x,y}$ was larger than the mean. Therefore, if a value of $\langle\tilde{u}\tilde{w}\rangle$ was derived from measurements over a particular area of the bed rather than over the whole measurement area, then it could misrepresent the unbiased form-induced stress. These observations on the spatial variability in $\tilde{u}\tilde{w}_{x,y}$ over the bed are supported by the results of *Aberle et al.* [2008] and *Campbell et al.* [2005] over gravel beds. These statistical errors are unlikely to have a large relative impact on the momentum budget within the upper part of the roughness layer, because the form-induced stress is much smaller than the Reynolds stress. But it may be more important closer to the roughness trough, where the form-induced stress becomes a more significant component of the momentum budget.

[36] The errors in estimating a spatially averaged flow variable and their change with measurement density are most significant at the lower densities. These lower densities are similar to those used by studies which have performed point velocity measurements. Furthermore, for some of the higher order flow parameters, the errors remained large close to the minimum required measurement density, owing to the high sensitivity that the error levels had with changes in measurement density. This indicates that careful consideration is required of the choice of measurement density when attempting to estimate the value of particular flow parameters. This could make it difficult to compare directly estimates made by studies that have used similar flow and bed conditions but different measurement densities.

5. Conclusions

[37] An examination has been made into the minimum density of measurements required to provide representative spatially averaged flow parameters over two water-worked gravel beds. This was coupled with an investigation into the influence of measurement density on the level of error in the estimation of these parameters. The results showed that of all the parameters investigated, the lowest density of velocity measurements was required to represent accurately the double-averaged streamwise velocity. The errors involved in sampling at lower density were not considerable. Twice the density was required for the turbulence intensities, and the implications of sampling at a lower density were more significant because large errors in estimates occurred even at densities only slightly lower than the required minimum. Much higher densities were required for the form-induced intensities and spatially averaged Reynolds stress; up to around double the density required for the turbulence intensities. It was shown that sampling at a lower measurement density will cause a very large under- and overestimation in form-induced intensity and spatially averaged Reynolds stress. In almost all cases, the maximum measurement density used in this study was required to provide a spatially representative estimate of form-induced stress. This is despite the measurements providing a high density of velocity measurements (relative to those studies using point velocity measurements). It revealed that larger densities and averaging areas are required for estimating form-induced stress. For all of the flow parameters, the level of error in adopting a lower measurement density than the required minimum, and its

change with measurement density, was especially large at the lower densities. Given this dependence on measurement density, caution should be taken when comparing flow estimates from studies that have used similar flow and bed conditions but different measurement densities.

[38] The minimum required measurement density for all of the spatially averaged flow parameters increased significantly within the roughness elements. For a particular parameter, the vertical profile shape and the minimum measurement density at a given height were reasonably consistent for the two beds at a similar level of relative submergence. For all but the double-averaged streamwise velocity, the minimum density at a given height decreased with a rise in relative submergence. Empirical relationships were developed across the range of submergences for the two beds which related minimum measurement density to relative height for a given level of precision and accuracy. The scaling with measurement height, flow length scale, and relative submergence suggested that it is appropriate to design a sampling strategy based on these relationships. This is likely to be valid for flows with mid- to high relative submergences and over macroscopically flat water-worked gravel beds which exhibit no significant bed forms. This approach only requires information on the geometric roughness height, bed shear velocity, and flow depth. No a priori detailed information is required on the temporal and spatial properties of the flow. The empirical relationships can be used to compare objectively data from different studies under similar bed and hydraulic conditions. It has also been shown how the choice of measurement density will influence the degree of spatial representation of the velocity measurements. It is possible to utilize these trends to estimate the required measurement density for a desired level of accuracy for similar flow and bed conditions. Further studies are required to investigate whether the empirical relationships can also be used for designing velocity sampling strategies and for comparing data from studies with beds of different surface topographies and flow conditions.

[39] **Acknowledgments.** The authors would like to thank the anonymous reviewers for their helpful and constructive comments.

References

Aberle, J. (2006), Spatially averaged near-bed flow field over rough armor layers, in *Proceedings of the International Conference on Fluvial Hydraulics, River Flow 2006*, vol. 1, edited by R. M. L. Ferreira, E. C. T. L. Alves, J. G. A. B. Leal, and A. H. Cardoso, pp. 153-162, Taylor & Francis, Oxford, UK.

Aberle, J. (2007), Measurements of armour layer roughness geometry function and porosity, *Acta Geophys.*, *55*(1), 23–32.

Aberle, J., and V. Nikora (2006), Statistical properties of armored gravel bed surfaces, *Water Resour. Res.*, *42*, W11414, doi:10.1029/2005WR004674.

Aberle, J., and G. M. Smart (2003), The influence of roughness structure on flow resistance on steep slopes, *J. Hydraul. Res.*, *41*(3), 259–269.

Aberle, J., K. Koll, and A. Dittrich (2007), Analysis of form induced stresses over rough gravel-bed armour layers, in *Proceedings of the XXXII IAHR Congress*, CD-ROM.

Aberle, J., K. Koll, and A. Dittrich (2008), Form induced stresses over rough gravel-beds, *Acta. Geophys.*, *56*(3), 584–600.

Ashworth, P. J., and R. I. Ferguson (1986), Interrelationships of channel processes, changes and sediments in a proglacial braided river, *Geogr. Ann. A*, *68*(4), 361–371.

Bouckaert, F. W., and J. Davis (1998), Microflow regimes and the distribution of macroinvertebrates around stream boulders, *Freshwater Biol.*, *40*(1), 77–86.

Boxall, J. B., and I. Guymer (2007), Longitudinal mixing in meandering channels: New experimental data set and verification of a predictive technique, *Water Res.*, *41*(2), 341–354.

Bridge, J. S., and J. Jarvis (1982), The dynamics of a river bend: A study in flow and sedimentary processes, *Sedimentology*, *29*(4), 499–541.

Buffin-Bélanger, T., A. G. Roy, and A. D. Kirkbride (2000), On large-scale flow structures in a gravel-bed river, *Geomorphology*, *32*(3–4), 417–435.

Buffin-Bélanger, T., S. Rice, I. Reid, and J. Lancaster (2006), Spatial heterogeneity of near-bed hydraulics above a patch of river gravel, *Water Resour. Res.*, *42*, W04413, doi:10.1029/2005WR004070.

Butler, J. B., S. N. Lane, and J. H. Chandler (2001), Characterization of the structure of river-bed gravels using two-dimensional fractal analysis, *Math. Geol.*, *33*(3), 301–330.

Butler, J. B., S. N. Lane, J. H. Chandler, and E. Porfiri (2002), Through–water close range digital photogrammetry in flume and field environments, *Photogramm. Rec.*, *17*(99), 419–439.

Campbell, L., I. McEwan, V. Nikora, D. Pokrajac, M. Gallagher, and C. Manes (2005), Bed-load effects on hydrodynamics of rough-bed open-channel flows, *J. Hydraul. Eng., ASCE*, *131*(7), 576–585.

Clifford, N. J., A. Robert, and K. S. Richards (1992), Estimation of flow resistance in gravel-bedded rivers: A physical explanation of the multiplier of roughness length, *Earth Surf. Proc. Land.*, *17*(2), 111–126.

Cooper, J. R. (2006), Spatially-induced momentum transfer over water-worked gravel beds, Ph.D. thesis, University of Sheffield, Sheffield, UK.

Cooper, J. R., and S. J. Tait (2008), The spatial organisation of time-averaged streamwise velocity and its correlation with the surface topography of water-worked gravel beds, *Acta Geophys.*, *56*(3), 614–641.

Cooper, J. R., and S. J. Tait (2009), Water-worked gravel beds in laboratory flumes: A natural analogue?, *Earth Surf. Proc. Land.*, *34*(3), 384–397.

Cooper, J. R., and S. J. Tait (2010), Examining the physical components of boundary shear stress for water-worked gravel deposits, *Earth Surf. Proc. Land.*, *35*(10), 1240–1246.

Ferreira, R. M. L., L. M. Ferreira, A. M. Ricardo, and M. J. Franca (2010), Impacts of sand transport on flow variables and dissolved oxygen in gravel-bed streams suitable for salmonid spawning, *River. Res. Appl.*, *26*(4), 414–438.

Furbish, D. J. (1987), Conditions for geometric similarity of coarse stream-bed roughness, *Math. Geol.*, *19*(4), 291–307.

Giménez-Curto, L. A., and M. A. Corniero (1996), Oscillating turbulent flow over very rough surfaces, *J. Geophys. Res.*, *101*(C9), 20,745–20,758, doi:10.1029/96JC01824.

Hardy, R. J., J. L. Best, S. N. Lane, and P. E. Carbonneau (2009), Coherent flow structures in a depth-limited flow over a gravel surface: The role of near-bed turbulence and influence of Reynolds number, *J. Geophys. Res.*, *114*, F01003, doi:10.1029/2007JF000970.

Hodge, R., J. Brasington, and K. Richards (2009), Analysing laser-scanned digital terrain models of gravel bed surfaces: Linking morphology to sediment transport processes and hydraulics, *Sedimentology*, *56*(7), 2024–2043.

Kironoto, B. A., and W. H. Graf (1994), Turbulence characteristics in rough uniform open-channel flow, *Proc. Instn. Civ. Engrs. Wat., Marit. Energy*, *106*(4), 333–344.

Koll, K. (2006), Parameterisation of the vertical velocity profile in the wall region over rough surfaces, in *Proceedings of the International Conference on Fluvial Hydraulics, River Flow 2006*, vol. 1, edited by R. M. L. Ferreira, E. C. T. L. Alves, J. G. A. B. Leal, and A. H. Cardoso, pp. 163–171, Taylor & Francis, Oxford, UK.

Koll, K., S. J. Tait, J. R. Cooper, J. Aberle, S. J. McLelland, B. J. Murphy, and G. Massaro (2008), Estimating flow turbulence characteristics over water-worked gravel beds using LDA and PIV measurement systems, in *Proceedings of the International Conference on Fluvial Hydraulics, River Flow 2008*, edited by M. Altinakar, M. A. Kokpinar, I. Aydin, S. Cokgor, and S. Kirkgöz, pp. 747–757, Kubaba Congr. Dep. and Travel Serv., Çeşme, Turkey.

Lamarre, H., and A. G. Roy (2005), Reach scale variability of turbulent flow characteristics in a gravel-bed river, *Geomorphology*, *68*(1–2), 95–113.

Lancaster, J., T. Buffin-Bélanger, I. Reid, and S. Rice (2006), Flow- and substratum-mediated movement by a stream insect, *Freshwater Biol.*, *51*(6), 1053–1069.

Lawless, M., and A. Robert (2001), Scales of boundary resistance in coarse-grained channels: Turbulent velocity profiles and implications, *Geomorphology*, *39*(3–4), 221–238.

Legleiter, C. J., T. L. Phelps, and E. E. Wohl (2007), Geostatistical analysis of the effects of stage and roughness on reach-scale spatial patterns of velocity and turbulence intensity, *Geomorphology*, *83*(3–4), 322–345.

Manes, C., D. Pokrajac, and I. McEwan (2007), Double-averaged open-channel flows with small relative submergence, *J. Hydraul. Eng., ASCE*, *133*(8), 896–904.

Marion, A., S. J. Tait, and I. K. McEwan (2003), Analysis of small-scale gravel bed topography during armoring, *Water Resour. Res.*, *39*(12), 1334, doi:10.1029/2003WR002367.

Matthaei, C. D., and H. Huber (2002), Microform bed clusters: are they preferred habitats for invertebrates in a flood-prone stream?, *Freshwater Biol.*, *47*(11), 2174–2190.

Mignot, E., E. Barthelemy, and D. Hurther (2009), Double-averaging analysis and local flow characterization of near-bed turbulence in gravel-bed channel flows, *J. Fluid Mech.*, *618*, 279–303.

Nezu, I., and H. Nakagawa (1993), *Turbulence in open channel flows*, A. A. Balkema, Rotterdam, Netherlands.

Nikora, V. I., D. G. Goring, and B. J. F. Biggs (1998), On gravel-bed roughness characterization, *Water Resour. Res.*, *34*(3), 517–527, doi:10.1029/97WR02886.

Nikora, V., D. Goring, I. McEwan, and G. Griffiths (2001), Spatially averaged open-channel flow over rough bed, *J. Hydraul. Eng., ASCE*, *127*(2), 123–133.

Nikora, V., K. Koll, I. McEwan, S. McLean, and A. Dittrich (2004), Velocity distribution in the roughness layer of rough-bed flows, *J. Hydraul. Eng., ASCE*, *130*(10), 1036–1042.

Nikora, V., S. McLean, S. Coleman, D. Pokrajac, I. McEwan, L. Campbell, J. Aberle, D. Clunie, and K. Koll (2007), Double-averaging concept for rough-bed open-channel and overland flows: Applications, *J. Hydraul. Eng., ASCE*, *133*(8), 884–895.

Packman, A., M. Salehin, and M. Zaramella (2004), Hyporheic exchange with gravel beds: basic hydrodynamic interactions and bedform-induced advective flows, *J. Hydraul. Eng., ASCE*, *130*(7), 647–656.

Pokrajac, D., L. J. Campbell, V. Nikora, C. Manes, and I. McEwan (2007), Quadrant analysis of persistent spatial velocity perturbations over square-bar roughness, *Exp. Fluids*, *42*(3), 413–423.

Radice, A., F. Ballio, and V. Nikora (2009), On statistical properties of bed load sediment concentration, *Water Resour. Res.*, *45*, W06501, doi:10.1029/2008WR007192.

Robert, A. (1988), Statistical properties of sediment bed profiles in alluvial channels, *Math. Geol.*, *20*(3), 205–225.

Robert, A. (1990), Boundary roughness in coarse-grained channels, *Prog. Phys. Geog.*, *14*(1), 42–70.

Robert, A. (1991), Fractal properties of simulated bed profiles in coarse-grained channels, *Math. Geol.*, *23*(3), 367–382.

Roy, A. G., T. Buffin-Belanger, H. Lamarre, and A. D. Kirkbride (2004), Size, shape and dynamics of large-scale turbulent flow structures in a gravel-bed river, *J. Fluid Mech.*, *500*, 1–27.

Sambrook Smith, G. H. S., and A. P. Nicholas (2005), Effect on flow structure of sand deposition on a gravel bed: results from a two-dimensional flume experiment, *Water Resour. Res.*, *41*, W10405, doi:10.1029/2004WR003817.

Shvidchenko, A. B., and G. Pender (2001), Macroturbulent structure of open-channel flow over gravel beds, *Water Resour. Res.*, *37*(3), 709–719, doi:10.1029/2000WR900280.

Smith, J. D., and S. R. Mclean (1977), Spatially averaged flow over a wavy surface, *J. Geophys. Res.*, *82*(12), 1735–1746, doi:10.1029/JC082i012p01735.

Song, T., U. Lemmin, and W. H. Graf (1994), Uniform-flow in open channels with movable gravel-bed, *J. Hydraul. Res.*, *32*(6), 861–876.

Tonina, D., and J. M. Buffington (2007), Hyporheic exchange in gravel bed rivers with pool-riffle morphology: Laboratory experiments and three-dimensional modeling, *Water Resour. Res.*, *43*(1), W01421, doi:10.1029/2005WR004328.

Wilson, N. R., and R. H. Shaw (1977), A higher-order closure model for canopy flow, *J. Appl. Meteorol.*, *16*(11), 1197–1205.

J. R. Cooper and S. J. Tait, School of Engineering, Design and Technology, University of Bradford, Richmond Rd., Bradford, BD7 1DP, UK. (J.Cooper2@Bradford.ac.uk)